

# Large-scale Numerical Simulations for Superconducting Neutron Detector using $\text{MgB}_2$ and Half Quantized Vortices in d-dot Array

Group Representative

Masahiko Machida Japan Atomic Energy Research Institute

Authors

Masahiko Machida <sup>\*1</sup> · Takuma Kano <sup>\*1</sup> · Susumu Yamada <sup>\*1</sup> · Tomio Koyama <sup>\*2</sup>

Masaru Kato <sup>\*3</sup>

\* 1 Japan Atomic Energy Research Institute

\* 2 Tohoku University

\* 3 Osaka Prefecture University

We performed large-scale numerical simulations for superconducting neutron detector using  $\text{MgB}_2$  by solving the time-dependent Ginzburg-Landau equation coupled with the Maxwell and the heat diffusion equation. The simulation results revealed that there is a threshold wire width for the neutron detection. On the other hand, we investigated patterns composed of several half quantized vortices seen in d-dot array embedded in the conventional superconductor matrix by solving the time-dependent Ginzburg-Landau equation considering the coupling between s and d-wave superconductors at the interface. With increasing the d-dot size, we found that possible patterns of half quantized vortices in a d-dot change from 2 diagonal patterns to 6 patterns including non-diagonal ones. These 6 patterns enable to create novel frustrated systems applicable to new devices.

**Keywords:** Superconducting neutron detector,  $\text{MgB}_2$ , half-quantized vortex, time-dependent Ginzburg-Landau equation

## I. Introduction

After the discovery of an alloy superconductor  $\text{MgB}_2$  [1], a quite unique application using  $\text{MgB}_2$  has been suggested by Ishida et al. in terms of neutron detection [2]. It is based on an intuitive idea that an energy released by a nuclear reaction between the neutron and  $^{10}\text{B}$  leads to an instantaneous destruction of the superconducting state and the moment is observable by the electrical signal generated in the nucleated normal regions [2]. In this paper, we investigate how the emerged hot normal region diffuses inside the superconductor and how the superconducting current-carrying states respond to the heat diffusion by performing direct numerical simulations [3] of the time-dependent Ginzburg-Landau (TDGL) equation coupled with the Maxwell and the heat diffusion equation [4].

Generally, the superconducting current with the zero resistance flows below the critical transition temperature ( $T_c$ ), while the current always requires a finite voltage above  $T_c$ . Thus, if the temperature is raised up above  $T_c$  by the neutron capture, then a voltage jump is expected to appear under the transport current. We clarify a condition required to observe the finite voltage jump after the energy release due to the neutron capture by the direct numerical simulations.

The symmetry of the superconducting order parameter of High- $T_c$  cuprate superconductors has been experimentally confirmed to be d-wave [5]. One of the most drastic confirmations was a direct evidence of the half vortex predicted to appear in grain boundaries induced on tri-crystalline substrates [6] and Josephson junctions between a conventional superconductor and  $\text{YBa}_2\text{Cu}_3\text{O}_7$ . Very recently, Hilgenkamp et al. constructed large scale arrays as zig-zag interfaces composed of d-wave and s-wave superconductors and reported ordering of several half vortices and their manipulations [7]. When a d-wave dot with a rectangular shape is embedded in a s-wave superconducting matrix, four half vortices are expected to appear spontaneously at the four corners of the d-dot. The emerged half vortices are insensitive to structural roughness produced through fabrication processes, and therefore, novel types of device applications including qu-bit can be expected [7].

Recently, many challenges toward the making of a qu-bit essential in the quantum computing have been made by using superconductors since the two level system constructed inside the superconducting gap have a great advantage in the context of very weak interference with environment. In fact, some groups have succeeded to manipulate their two

level systems in a quantum manner by using the charging effect [8] and the fluxon [9]. These ways have been called the superconducting charge qubit [8] and flux qubit [9], respectively. In contrast to such a fashion, we explore another way in this paper. The way is to create useful frustrated systems based on classical computing concepts by arranging large-scale d-dots in array manners. Our studies on d-dot in terms of qubit are described elsewhere [10].

The numerical simulation techniques and their results for the neutron devices are given in Section II. The simulation method for d-dot arrays and their results for the patterns composed of half quantized vortices are presented in Section III. Finally, summary and discussion are given in the last section.

## II. Large-scale Simulations for the Neutron Detectors using $\text{MgB}_2$

In order to simulate the dynamics of the superconducting state and the temperature after the neutron capturing in  $\text{MgB}_2$ , we solve the TDGL equation coupled with the Maxwell [3] and the heat diffusion equation [4]. The TDGL and the Maxwell equation describe the dynamics of the superconducting order parameter and the vector potential, respectively. First, the TDGL equation is given as follows,

$$D^{-1} \left\{ \frac{\partial}{\partial t} + i \frac{2e\phi}{\hbar} \right\} \Delta = -\xi^{-2} (|\Delta|^2 - 1) \Delta - \left\{ \frac{\Delta}{i} - \frac{2e}{\hbar c} \mathbf{A} \right\} \Delta = 0 \quad (1),$$

where  $D$ ,  $\phi$ ,  $\xi$ , and  $\lambda$  are the diffusion constant, the scalar potential, the coherence length, and the magnetic penetration depth, respectively.  $\Delta$  is the complex order parameter and  $\mathbf{A}$  is the vector potential whose dynamics are described by the Maxwell equation,

$$\nabla \times \mathbf{B} = \frac{4\pi}{c} \mathbf{j} \quad (2),$$

where the current density is given by

$$\mathbf{j} = \sigma \left\{ -\nabla\phi - \frac{1}{c} \frac{\partial \mathbf{A}}{\partial t} \right\} + \text{Re} \left[ \Delta^* \left\{ \frac{\nabla}{i} - \frac{2e}{\hbar c} \mathbf{A} \right\} \Delta \right] \frac{\hbar c^2}{8\pi e} \lambda^{-2},$$

where  $\sigma$  is the normal conductivity and the first and the second terms stand for the normal and the superconducting current components, respectively. In order to realize the temperature change after the energy release due to the nuclear reaction between neutron and  $^{10}\text{B}$ , we must trace the heat diffusion process with the superconducting state dynamics. For the purpose, we use the energy conservation law which gives a balance between the energy dissipation as the Joule heat and the heat flow decomposed into the superconducting and the normal components. The equation is given by

$$C_v \frac{dT}{dt} + \frac{dF_s}{dt} + \text{div} \left( \mathbf{j}_n^Q + \mathbf{j}_s^Q \right) + W = 0 \quad (3),$$

where  $C_v$ ,  $F_s$ , and  $W$  are the heat capacity, the GL Free energy, and the Joule heat, respectively, and  $\mathbf{j}_n^Q$  and  $\mathbf{j}_s^Q$  are the

normal and the superconducting heat currents. By solving the equation, we can simulate the time development of the local temperature  $T$ . The heat released by the nuclear reaction is added to the right hand side of Eq. (3) only at the neutron captured spot which is assumed to be a tiny region limited within a few tens of the coherence length. In the future, the spots in which the energy is released will be dealt with in more details by considering the flight of  $\alpha$  particle inside the matter. In the present simulation, the superconducting order parameter, the vector potential, and the temperature are simultaneously computed under the above initial condition and the superconductivity destruction processes with the heat diffusion from the hot-spot are traced.

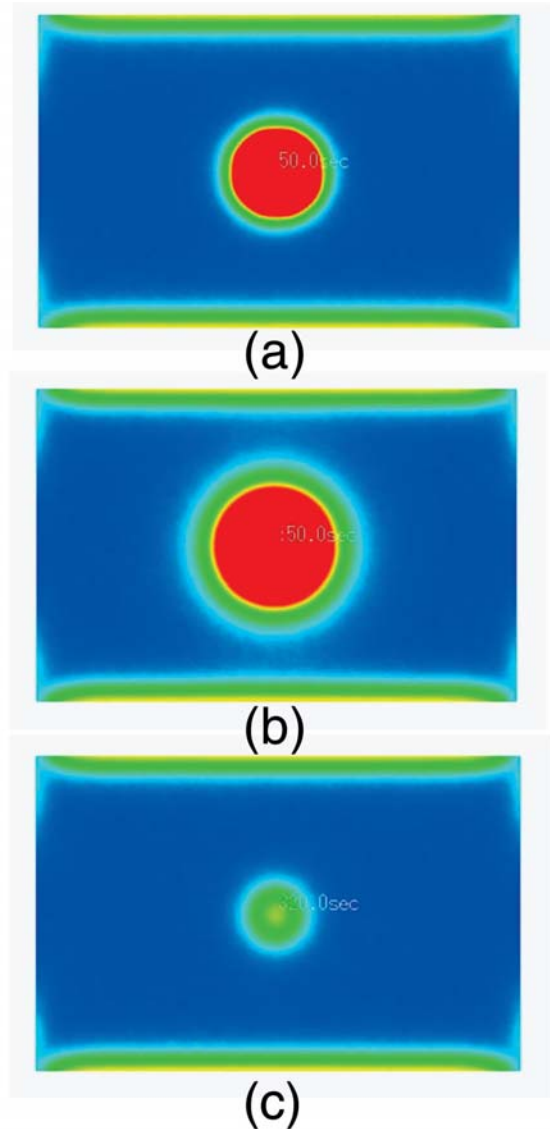


Fig. 1 The three snapshots for the distribution of the superconducting order parameter. These display the dynamics of the hot-spot nucleated by the neutron capture in  $\text{MgB}_2$  superconducting wire where the current is applied from the left to the right hand side. (a) The initial stage just after the nucleation of the hot-spot. (b) The intermediate stage. The size of the normal region located at the center is the maximum. (c) The last stage. The hot spot is quenched and the normal region shrinks.

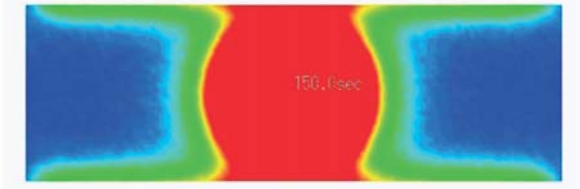


Fig. 2 The snapshot of the superconducting order parameter distribution. The hot-spot extends from an edge to another one.

Let us present typical simulation results and discuss a critical condition for the neutron detection. Figure 1 (a) is a snapshot of the order parameter amplitude  $\Delta$  at the initial stage just after the neutron is captured at the center of the wire region whose width is about  $40 \xi$  ( $T = 0$ ), where  $\xi$  ( $T = 0$ )  $\sim 5$  nm. The superconducting order parameter is found to be strongly suppressed in the circular spot region at the center. This means that the region changes into the normal state. After the initial heat release and the local superconductivity destruction, the heat further propagates and the normal region enlarges as seen in Fig. 1 (b) where the size of the normal region is the maximum. Here, we note that the cool heat bath always quenches the superconductor from the all surfaces in order to keep the temperature of  $\text{MgB}_2$  superconductor constant. Thus,  $\text{MgB}_2$  warmed up after the neutron capture is quenched up to the same temperature in the initial state at the final stage. The result of the disappearance of the normal hot-spot is seen in Fig. 1 (c).

Here, we demonstrate that there is a threshold wire width for the neutron detection. In the time sequence of Fig. 1, we suggest that the superconducting current can flow even in Fig. 1 (b) where the size of the normal hot-spot is the maximum. This means that the neutron can not be detected in such a wide wire. On the other hand, if we decreases the width up to the size as shown in Fig. 2, then, the normal region is found to extend from an edge to another one. Only in this situation, the voltage jump becomes observable. Thus, we find that there is a width threshold to detect the neutron enough. This is a quite important information for the device construction.

### III. Large-scale Simulations for d-dot Arrays Embedded in s-wave Superconductor

The symmetry of the order parameter of cuprate High- $T_c$  superconductors is well-known to be d-wave, while that of the conventional ones is usually s-wave. Thus, if a square shape dot of High- $T_c$  superconductor is embedded in the conventional superconductor matrix, then the interference effects between different signs of the order parameters occur at the interface. The coupling free energy at the interface is given by

$$F_t = t_x (\Delta_s \Delta_d e^{iA_{sd}} + c.c.) - t_y (\Delta_s \Delta_d e^{iA_{sd}} + c.c.)$$

where  $t$  is the coupling constant between both superconductors

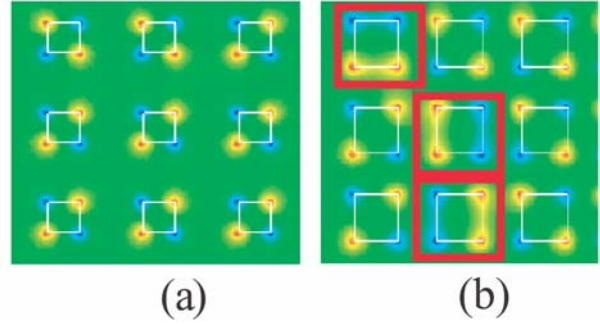


Fig. 3 The magnetic field distribution for d-dot array embedded in the conventional superconductor matrix. (a) The small d-dot array. (b) The large d-dot array. The d-dots surrounded by the red line show non-diagonal pattern of half vortices.

tors and the sign of the coefficient is different depending on the crystal axes. In the expression, it is found that  $\pi$  and 0 phase differences are favored along the x- and the y-directions, respectively. In this paper, we perform the numerical simulations for the TDGL and the Maxwell equations considering the above coupling energy in addition to the usual Ginzburg-Landau free energy. Typical simulation results are given in Fig. 3 (a) and (b) where the size dependence of d-dots on the distributions of half and anti-half quantized vortices is demonstrated. Those figures show the snapshots of the magnetic field distributions in which the white line indicates the interface between the different superconductors and the red and blue colors the represent the maximum of the positive and the negative values of the magnetic field magnitude, respectively. In these figures, it is found that only the diagonal patterns of the half and anti-half quantized vortices are observable in the case of the relatively small d-dot (Fig. 3 (a)) while the non-diagonal patterns which are surrounded by the red lines also emerge in the case of the relatively large d-dots (Fig. 3(b)). The reason is as follows. The magnetic interaction between half quantized vortices with the same polarities is repulsive and those with opposite polarities are attractive. The former case gives the free energy increase, while the latter case results in the free energy decrease. Thus, in order to reduce the magnetic energy as much as possible the diagonal patterns are found to be favored in cases of the small d-dot. On the other hand, the magnetic interaction energy between the half vortices become negligible small in the case of the dot whose size is larger than the penetration depth. Then, all possible 6 patterns seen in Fig. 3(b) can emerge.

Now, let us study which kind of frustrated systems can be created by using 6 patterns. As an interesting example, we suggest that the zigzag d-dot array as seen in Fig. 4 (a) gives 2D spin-ice in which 2-in and 2-out rule holds inside the unit component seen in Fig. 4 (b). This result means that we can approach useful frustrated systems by arranging d-dots in proper manners.

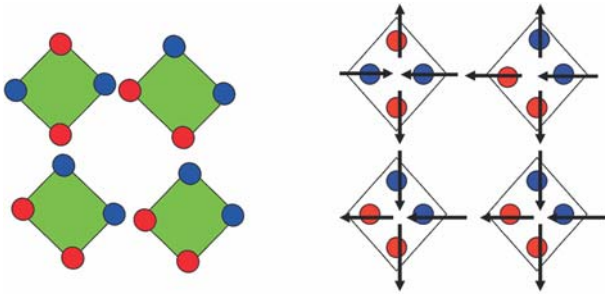


Fig. 4 (a) The zigzag array of d-dot. (b) The equivalent schematic figure of the pattern of half vortices emerged in the proposed array configuration (a). It is found in the configuration that the 2-in and 2-out rule holds inside the d-dot unit.

#### IV. Summary and Conclusion

We performed large scale simulations for two kinds of superconducting devices, one of which is the neutron detector using  $\text{MgB}_2$  and another of which is the novel device using manipulations of half quantized vortices emerged spontaneously by embedding High- $T_c$  d-dot in the conventional superconductor matrix. In terms of the neutron detector, we gave a rough estimation on the threshold wire width for the neutron detection. In the High- $T_c$  d-dot, we confirmed that useful frustrated systems like 2D spin ice can be constructed by arranging d-dots in the zigzag manner.

#### References

- [1] J. Nagamatsu, N. Nakagawa, T. Muranaka, Y. Zenitani, and J. Akimitsu, *Nature* **410**, 63(2001).
- [2] K. Takahashi, K. Satoh, T. Yotsuya, S. Okayasu, K. Hojou, M. Katagiri, A. Saito, A. Kawakami, H. Shimakage, Z. Wang, and T. Ishida, *Physica C* **392–396**, 1501(2003).
- [3] M. Machida and H. Kaburaki, *Phys. Rev. Lett.* **75**, 3178(1995); M. Machida, A. Tanaka, and M. Tachiki, *Physica C* **288**, 199(1997).
- [4] I. Shapiro, E. Pechenik, and B. Ya. Shapiro, *Phys. Rev. B* **63**, 184520(2001).
- [5] See, C. C. Tsuei and J. R. Kirtley, *Rev. Mod. Phys.* **72**, 969(2000) and many references therein.
- [6] See, D. J. Harlingen, *Rev. Mod. Phys.* **67**, 515(1995).
- [7] H. Hilgenkamp et al., *Nature* **422**, 50(2003).
- [8] See, Y. Nakamura et al., *Phys. Rev. Lett.* **88**, 047901(2002).
- [9] See, J. E. Mooij et al., *Science*, 285, 1036(1999).
- [10] M. Machida, T. Koyama, M. Kato, and T. Ishida, *Physica C* (To be published).